Development of a Finite-Temperature Density Functional Approach to Electrochemical Reactions

Kazuya Shiratori[†] **and Katsuyuki Nobusada***[,†,‡]

Department of Structural Molecular Science, The Graduate University for Advanced Studies, Okazaki 444-8585, Japan, and Department of Theoretical and Computational Molecular Science, Institute for Molecular Science, Okazaki 444-8585, Japan

Received: May 4, 2008; Revised Manuscript Received: July 18, 2008

We present a computational method to calculate the electronic states of a molecule in an electrochemical environment. The method is based on our recently developed finite-temperature density functional theory approach to calculate the electronic structures at a constant chemical potential. A solvent effect is treated at the level of the extended self-consistent reaction field model, which allows considering a nonequilibrium solvation effect. An exchange-correlation functional with a long-range correction is employed in this calculation, because the functional is adjusted so that the derivative discontinuity of energy with respect to a number of electrons could be satisfied. It has been found that the derivative discontinuity condition plays a crucial role in an electrochemical system. The computational results are presented for a reaction of $NO^+ + e^- \rightleftarrows NO$ in chemical equilibrium. Owing to the improvement in the solvation effect and the exchange-correlation functional, the calculated activation free energy is in good agreement with experimental results.

1. Introduction

Electrochemical processes have received significant attention in a wide range of interest in the electrochemical cell, corrosion, and membrane potential.[1,2] Their importance has extensively been recognized in recent years, for example, in the context of energy conversion related to photoelectrochemical cells based on advanced fabrication technology.[2] All of the electrochemical processes are, in a narrow sense, due to the details of the electronic structures of a system in electrochemical environment. Nevertheless, it is still computationally demanding to carry out first-principles calculations of such electronic states. This is simply because reactant−solvent and reactant−electrode interactions, which are completely absent in isolated molecular systems, play an important role. Therefore, the electrochemical processes have so far been studied within various numerical models at different levels of theory depending on the description of those interactions. In addition, one encounters serious difficulty in calculating the electronic structures of an electrochemical system. Since the electrochemical system is an open quantum one, that is, a molecular system in contact with an electrode, the electronic structure calculations of such a system should be carried out at a constant chemical potential, μ, instead of a fixed number of electrons, N.

The conventional ab initio calculations such as quantum chemistry or band structure give electronic structures at a constant N. However, N is no longer a suitable variable in electrochemical processes at a constant μ. For this reason, several approaches have been developed to calculate electronic structures at a constant chemical potential.[3−19] Sprik et al.[3−6] and Anderson et al.[7−10] proposed methods to calculate the electronic structure at a constant μ on the basis of the conventional ab initio calculations. On the other hand, Nakatsuji et al.[11−13] developed a method of electronic structure calculations at a constant μ in a different way. This method was used to improve the accuracy of the conventional cluster model calculation, which is frequently applied to electronic structure calculations of adsorbate−surface systems. In this method, however, μ was calculated as a derivative of the total energy with respect to N, so that a large number of calculations were needed to obtain the electronic state at a desired μ.

The disadvantage of the computations mentioned above is ascribed to the fact that these numerical methods are still based on electronic structure calculations of a system with a constant N. Therefore, it is highly desirable to develop an alternative method to directly calculate electronic structures at a constant μ.[15−19] Finite-temperature density functional theory (FTDFT)[20] is in principle able to treat a system in a grand canonical ensemble average, and thus, one can propose a numerical method based on FTDFT to describe electrochemical processes. Alavi et al.[15] applied the FTDFT method to the simulation of charged slabs at a constant μ. Their procedure allowed performing calculations for an electrochemical system by using the standard ab initio supercell approach. In their study, however, the artificial compensating charge was introduced because the net charge in the supercell should be neutralized in the band structure calculation. Otani and Sugino[18] proposed a different method of the band structure calculation for an electrochemical system in which the charge neutrality was satisfied by imposing an appropriate boundary condition on a Poisson equation.

Very recently, we have developed an alternative FTDFT method to calculate the electronic structures of an electrochemical system at a constant μ.[19] In contrast to the band structure calculations mentioned above, our method is based on the conventional quantum chemistry calculations. Thus, the method requires no charge neutrality condition and allows us to intuitively understand chemical processes. Our FTDFT approach has qualitatively calculated the electronic structures at a constant μ, whereas it should be further improved. Specifically, there remain two problems to be addressed.

* Corresponding author, nobusada@ims.ac.jp.
† The Graduate University for Advanced Studies.
‡ Institute for Molecular Science.

10.1021/jp803923f CCC: $40.75
Published on Web 10/01/2008

First, in our previous study, we primarily focused on developing an FTDFT approach to calculate electronic structures at a constant μ. The solvation effect was simply approximated by a conductor-like polarizable continuum model (C-PCM).[21] This treatment means that the solvent is assumed to be in equilibrium with the solute. In the electrochemical process accompanying electron transfer, however, such an equilibrium condition is no longer satisfied because the solvent motion is in general much slower than the electron transfer.

Second, the conventional functional, the Becke three-parameter hybrid exchange functional with the Lee−Yang−Parr correlation functional (B3LYP), was used in our previous FTDFT approach. In the extension of the Hohenberg−Kohn theorem to the system with a fractional number of electrons N by Perdew et al.,[22] they demonstrated that the energy calculated by using DFT should show derivative discontinuity with respect to N. Although the importance of the derivative discontinuity condition was pointed out in our previous study[19] and it is known that the B3LYP functional does not reproduce this condition, we had no detailed discussion about the improvement in the functional.

In the present study, we further develop the FTDFT approach to analyze the kinetics of electrochemical processes. We adopt the extended self-consistent reaction field (SCRF) model,[23,24] which allows us to take account of the nonequilibrium solvation effect. We alternatively employ the Becke exchange and Lee−Yang−Parr correlation functional with a long-range correction (LC-BLYP) and discuss the importance of the derivative discontinuity with respect to the number of electrons. The approach is applied to the reaction of $NO^+ + e^- \rightleftarrows NO$ in acetonitrile.[25]

This paper is organized as follows. In section 2, we describe the FTDFT method combined with the SCRF model. The computational details, including the description of LC-BLYP, are presented in section 3. In section 4, we show the results of the calculation for the reaction of $NO^+ + e^- \rightleftarrows NO$. The concluding remarks are summarized in section 5.

2. Methods

2.1. FTDFT Calculation. In our previous study, we calculated the electronic structures at a constant μ in a direct manner. The computational approach is based on FTDFT. We review here the FTDFT approach.

FTDFT is a generalization of DFT[26] to a grand canonical ensemble first developed by Mermin,[20] extending the Hohenberg−Kohn theorem.[27] The density operator $\hat{\Gamma}$ at the equilibrium state for a grand canonical ensemble minimizes the grand potential $\Omega[\hat{\Gamma}]$. According to FTDFT, Ω can be given by a functional form of electron density n instead of $\hat{\Gamma}$ as follows:

$$\Omega[n(\mathbf{x})] = E - \theta S - \mu N \quad (1)$$

$$= T[n(\mathbf{x})] + V_{ee}[n(\mathbf{x})] - \theta S[n(\mathbf{x})] + \int (v(\mathbf{x}) - \mu) n(\mathbf{x})\, d\mathbf{x} \quad (2)$$

where E, T, and V_{ee} are internal, kinetic, and electron−electron interaction energies, respectively, S is entropy, θ is temperature, and v is external potential. In the Kohn−Sham (KS) formulation, as is well-known, a system of interacting electrons is represented by a fictitious system of noninteracting electrons. Similarly, Ω can be rewritten by

$$\Omega[n(\mathbf{x})] = T_s[n(\mathbf{x})] + J[n(\mathbf{x})] - \theta S_s[n(\mathbf{x})] + \int (v(\mathbf{x}) - \mu) n(\mathbf{x})\, d\mathbf{x} + \Omega_{xc}[n(\mathbf{x})] \quad (3)$$

where

$$n(\mathbf{x}) = \sum_i^{\infty} f_i |\psi_i(\mathbf{x})|^2 \quad (4)$$

$$T_s[n] = \sum_i^{\infty} f_i \int \psi_i^*(\mathbf{x}) \left(-\frac{1}{2}\nabla^2\right) \psi_i(\mathbf{x})\, d\mathbf{x} \quad (5)$$

$$J[n] = \frac{1}{2} \int \int \frac{n(\mathbf{x}) n(\mathbf{x}')}{|\mathbf{x} - \mathbf{x}'|}\, d\mathbf{x}\, d\mathbf{x}' \quad (6)$$

$$S_s[n] = -k_B \sum_i^{\infty} \{f_i \ln f_i + (1 - f_i) \ln(1 - f_i)\} \quad (7)$$

with ψ_i and f_i being the KS orbitals and the occupation numbers, respectively, and k_B being the Boltzmann's constant. $\Omega_{xc}[n]$ is an exchange-correlation contribution to the grand potential and it is expressed by $\Omega_{xc} = (T - \theta S) - (T_s - \theta S_s) + V_{ee} - J$. Finally, the KS equation at finite temperature is derived in the form of[28]

$$\hat{h}_{eff}^{\ 0} \psi_i(\mathbf{x}) = \varepsilon_i \psi_i(\mathbf{x}) \quad (8)$$

where $\hat{h}_{eff}^{\ 0}$ is the effective one-electron Hamiltonian given by

$$\hat{h}_{eff}^{\ 0} = -\frac{1}{2}\nabla^2 + \int \frac{n(\mathbf{x}')}{|\mathbf{x} - \mathbf{x}'|}\, d\mathbf{x}' + v_{xc}(\mathbf{x}) + v(\mathbf{x}) \quad (9)$$

with $v_{xc}(\mathbf{x})$ being the exchange-correlation potential and ε_i being the KS orbital energies. It should be noted here that $\mathbf{v}_{xc}(\mathbf{x})$ is not the conventional exchange-correlation potential but the exchange-correlation potential for the ground potential given in FTDFT. Equation 8 is formally equivalent to the conventional KS equation at zero temperature, but the electron density $n(\mathbf{x})$ depends on temperature through the fractional occupation numbers f_i as written in the form of eq 4. f_i in the noninteracting electron system equals to the Fermi−Dirac distribution

$$f_i = \frac{1}{1 + \exp\left(\frac{\varepsilon_i - \mu}{k_B \theta}\right)} \quad (10)$$

Once one solves the FTDFT equation (eq 8), satisfying eqs 4 and 10 in the same way as in the conventional KSDFT approach, the equilibrium electron density at μ, θ, and v is obtained.

In the present modeling of electrochemical systems, we assume an outer-sphere process in which an electrode is considered to be an electron reservoir associated with a chemical potential μ. Thus, we do not explicitly calculate the interaction between reactant molecules and an electrode. The energy of an electron is experimentally measured in terms of an electrode potential ν relative to a reference electrode. In the FTDFT calculation, the energy of an electron is measured in terms of chemical potential μ in which an electron in the vacuum at rest is defined as zero. Then, μ and ν are related by

$$\nu = -\frac{\mu}{e} - 4.36 \text{ V vs SHE} \quad (11)$$

where e is the elementary charge and the standard hydrogen electrode (SHE) is assumed as the reference electrode. This relationship will be derived in Appendix A.

The FTDFT approach described above is similar to the conventional KSDFT except that the former approach requires an extra (but not computationally demanding) procedure to

specify the fractional occupation numbers. Therefore, the FTDFT approach can be straightforwardly implemented to standard quantum chemistry programs.

2.2. SCRF Model for Nonequilibrium Solvation. The solvation effect was simply approximated by C-PCM in our previous method. As mentioned in section 1, this approximation ignores the nonequilibrium solvation effect. We herein take account of the nonequilibrium solvation effect by using the extended SCRF model.[23,24]

The system is assumed to be in a spherical cavity embedded in a dielectric. The energy difference ΔE between the molecule in the vacuum and the molecule in the dielectric can be expressed as[23]

$$\Delta E = -\frac{1}{2} f_q^{\,0} q^2 - \frac{1}{2} f_m^{\,0} \mathbf{m} \cdot \mathbf{m} \tag{12}$$

where q and $\mathbf{m}$ are, respectively, the charge and the dipole moment vector of the molecule, and $f_q^{\,0}$ and $f_m^{\,0}$ are the reaction field factors for the charge and the dipole moment. q and $\mathbf{m}$ are calculated by the FTDFT calculation described above. The reaction field factors are given by

$$f_q^{\,0} = \left(1 - \frac{1}{\varepsilon_0}\right)\frac{1}{a_0} \tag{13}$$

$$f_m^{\,0} = \frac{2(\varepsilon_0 - 1)}{2\varepsilon_0 + 1}\frac{1}{a_0^{\,3}}$$

where a_0 is the radius of the spherical cavity and ε_0 is the dielectric constant. Although only the contributions from the charge and the dipole moment are discussed in the present study, the contributions from higher multipole moments can be similarly taken into account.

If the charge distribution of a solute molecule changes fast, solvent is no longer in equilibrium with the solute molecule. We divide the solvent polarization into a long-lived (inertial) component and a short-lived (noninertial) component. Then, we assume the long-lived component is frozen at the polarization produced by a charge q^0 and a dipole moment $\mathbf{m}^0$, and the short-lived component has an instantaneous response to the change in the charge distribution of the solute molecule. On this assumption, ΔE is rewritten as (see Appendix B)

$$\Delta E = \frac{1}{2}(f_q^{\,0} - f_q^{\,\infty})(q^0)^2 - \frac{1}{2} f_q^{\,\infty} q^2 - (f_q^{\,0} - f_q^{\,\infty}) q (q^0) +$$

$$\frac{1}{2}(f_m^{\,0} - f_m^{\,\infty})\mathbf{m}^0 \cdot \mathbf{m}^0 - \frac{1}{2} f_m^{\,\infty} \mathbf{m} \cdot \mathbf{m} - (f_m^{\,0} - f_m^{\,\infty})\mathbf{m} \cdot \mathbf{m}^0 \tag{14}$$

where $f_q^{\,\infty}$ and $f_m^{\,\infty}$ are the reaction field factors of the short-lived components for the charge and the dipole moment, respectively. These reaction field factors are given by

$$f_q^{\,\infty} = \left(1 - \frac{1}{n^2}\right)\frac{1}{a_0} \tag{15}$$

$$f_m^{\,\infty} = \frac{2(n^2 - 1)}{2n^2 + 1}\frac{1}{a_0^3}$$

with n being the refractive index of the dielectric. The radii for the long-lived component and the short-lived component are taken to be equal.[29,30]

To calculate the electronic structures in electrochemical environment, ΔE should be added to the grand potential Ω given by eq 3. Then, the finite-temperature KS equation (eq 8) is simply modified in the form of (see Appendix C)

$$\hat{h}_{\mathrm{eff}} \psi_i(\mathbf{x}) = \varepsilon_i \psi_i(\mathbf{x}) \tag{16}$$

where

$$\hat{h}_{\mathrm{eff}} = \hat{h}_{\mathrm{eff}}^{\,0} + v_{\mathrm{scrf}} \tag{17}$$

$$v_{\mathrm{scrf}} = -[f_q^{\,\infty} q \hat{q} + (f_q^{\,0} - f_q^{\,\infty}) q^0 \hat{q} + f_m^{\,\infty} \mathbf{m} \cdot \hat{\mathbf{m}} +$$

$$(f_m^{\,0} - f_m^{\,\infty})\mathbf{m}^0 \cdot \hat{\mathbf{m}}] \tag{18}$$

with $\hat{q}$ and $\hat{\mathbf{m}}$ being the operators for the charge and the dipole moment, respectively. Equation 16 is the final form of our FTDFT approach combined with the extended SCRF model. The equation is calculated until v_{scrf}, q, and $\mathbf{m}$ are determined self-consistently.

The long-lived component of the polarization is associated with the atomic configuration of the solvent, whereas the short-lived component is due to the distribution of the electron density. Thus, the variables of q^0 and $\mathbf{m}^0$, which determine the long-lived component of the polarization, can be interpreted to specify the solvent structure.[24] To approximately specify the solvent structure on the reaction coordinate, we determine the variables, q^0 and $\mathbf{m}^0$, by linearly interpolating the charges and the dipole moments in the neutral (N) and cationic (C) states

$$q^0(S) = (1 - S) q^{\mathrm{N}} + S q^{\mathrm{C}} \tag{19}$$

$$\mathbf{m}^0(S) = (1 - S)\mathbf{m}^{\mathrm{N}} + S\mathbf{m}^{\mathrm{C}} \tag{20}$$

where S is a reduced index related to the atomic coordinate of the solvent molecules. In what follows, we refer to S as the solvent coordinate.

3. Computational Details

The exchange-correlation potential $v_{\mathrm{xc}}(\mathbf{x})$ in eq 9 is approximated by the Becke exchange[31] and Lee−Yang−Parr correlation functional[32] with a long-range correction (LC-BLYP).[33−35] The temperature dependence of the functional is ignored. The Coulomb operator in LC-BLYP is decomposed into short-range and long-range parts by a parameter ω.[36,37] The exchange energy in the short-range part is calculated by the BLYP functional and that of the long-range part is calculated by the Hartree−Fock (HF) exchange potential. The optimum value of ω should be between 0 (the HF limit) and ∞ (the BLYP limit). In the present calculation, the parameter ω was optimized to be 0.31. The choice of the optimum value of ω will be discussed in section 4.2. The KS orbitals are expanded in Dunning's augmented correlation-consistent basis set (aug-cc-pVDZ).[38,39] The dielectric constant and the square of the refractive index of acetonitrile in the SCRF model are set to be 37.5 and 1.8, respectively.[40] The calculations are carried out with the GAMESS package of quantum chemistry programs[41] in which the present computational FTDFT/SCRF methodology is implemented. The radius r of the cavity in the SCRF model is calculated to be 2.091 Å by the equation

$$r = \frac{1}{2}[r^{\mathrm{vdW}}(\mathrm{N}) + r^{\mathrm{vdW}}(\mathrm{O}) + \frac{1}{2}\{R_{\mathrm{eq}}(\mathrm{NO}) + R_{\mathrm{eq}}(\mathrm{NO}^+)\}] \tag{21}$$

where $r^{\mathrm{vdW}}(\mathrm{N})$ and $r^{\mathrm{vdW}}(\mathrm{O})$ are the van der Waals radii[42] of N and O, respectively, and $R_{\mathrm{eq}}(\mathrm{NO})$ and $R_{\mathrm{eq}}(\mathrm{NO}^+)$ are the equilibrium internuclear distances obtained by the DFT calculation in a vacuum with LC-BLYP ($\omega = 0.31$) and the aug-cc-pVDZ basis set.

To calculate the electronic states at a given μ, we first carry out electronic structure calculations at a constant N and then

TABLE 1: Properties of NO and NO^+[a]

	R_{eq} (Å)	q_e (a.u.)	q_n (a.u.)	m_e (a.u.)	m_n (a.u.)	E_{total} (eV)
NO	1.1524	−15.0	15.0	1.003	−1.089	−3528.759
NO^+	1.0704	−14.0	15.0	1.198	−1.011	−3522.422

[a] R_{eq} is the equilibrium internuclear distance, q_e and q_n are the charges of electrons and nuclei, m_e and m_n are the dipole moments of electrons and nuclei along the molecular axis of the system, and E_{total} is the total energy. The origin of the dipole moment is the center of the internuclear coordinate between N and O.

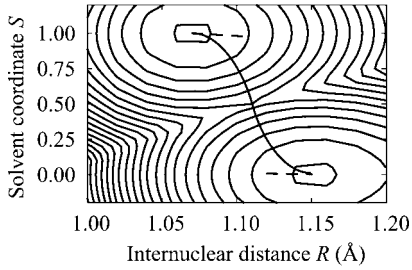

Figure 1. Grand potential surface of $NO^+ + e^- \rightleftarrows NO$ at the standard electrode potential. The solid and dashed lines show the reaction coordinates when the nonequilibrium solvation is taken into account and not taken into account, respectively.

evaluate the chemical potential. This computation is repeated until the electronic state at the desired μ is obtained, i.e., a route search computation.[19] It is not necessarily the case that there is a one-to-one mapping between the electronic states at μ and N. Thus, multivalued electronic states are sometimes artificially obtained for the desired μ. As will be described later, this practical problem can be avoided by using a proper exchange-correlation potential in FTDFT calculations.

4. Results and Discussion

4.1. Grand Potential Surface. The properties of NO and NO^+ in equilibrium with acetonitrile are summarized in Table 1. The difference in the energy between NO and NO^+, $-3528.759 - (-3522.422) = -6.337$ eV, is equal to the chemical potential at the electrochemical equilibrium condition, $NO^+ + e^- \rightleftarrows NO$. Thus, the standard electrode potential of this reaction is calculated to be $(-(-6.337) - 4.36)) \simeq 1.98$ V vs SHE from eq 11. The experimental redox potential is 1.52 V vs SHE.[25] The computational error is mainly due to the incompleteness of the solvation model in which the solvent is represented by a dielectric and might be due to the inaccuracy caused by the DFT approach.

Figure 1 shows the grand potential surface as a function of the internuclear distance R and the solvent coordinate S at the standard electrode potential, 1.98 V vs SHE. The solvent coordinate was determined by using eqs 19 and 20 with the data in Table 1. A double minimum can be seen in the figure: the minimum in the cationic (NO^+) state at $R = 1.0704$ Å and $S = 1.0$, and the minimum in the neutral (NO) state at $R = 1.1524$ Å and $S = 0.0$. The saddle point appears at $R = 1.1096$ Å and $S = 0.493$, and the activation free energy is calculated to be 12.17 kcal/mol. This value is in good agreement with an experimental result of 11 kcal/mol.[25]

The reaction path connecting the two potential minimums is drawn in Figure 1 (the solid curve). For comparison, we also draw the "false" reaction path obtained when the equilibrium solvation is assumed (the dotted lines extending from both of the potential minimums). It should be noted that this false path is a function of R and the degree of freedom of the solvent coordinate is completely ignored even though the path is drawn

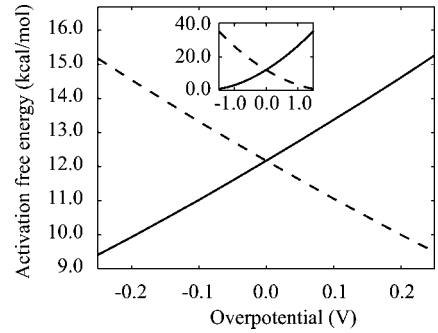

Figure 2. Activation free energy as a function of the overpotential. The solid and dashed lines show the energies of the reduction, $NO^+ + e^- \rightarrow NO$, and the oxidation, $NO^+ + e^- \leftarrow NO$. The inset shows the activation free energy in a wider range of the overpotential.

in the 2D (R and S) map. Thus, the 1D false reaction path jumps unreasonably from one end to another. This unphysical jump gives the inaccurate value of the activation free energy, ≃3 kcal/mol. The effect of the nonequilibrium solvation plays a crucial role in the kinetics of electrochemical reactions.

As is well-known in the Butler−Volmer equation or the Tafel relationship, the activation free energy has approximately linear dependence on overpotential η. Therefore, the activation free energy of the reduction, $NO^+ + e^- \rightarrow NO$, should linearly increase as a function of the overpotential, whereas that of the oxidation, $NO^+ + e^- \leftarrow NO$, should linearly decrease. Figure 2 shows the activation free energy as a function of η. The figure reasonably demonstrates that the dependence of the activation free energy on the overpotential satisfies the requirements mentioned above.

We discuss here the nonequilibrium solvation dynamics based on the SCRF model in relationship to Marcus theory. According to Marcus theory, diabatic free energy curves along the reaction coordinate are assumed to be parabolic. Thus, we drew the NO/NO^+ diabatic potential curves by fitting the grand potential along the minimum energy path to two parabolic curves. The barrier height at the crossing point of the two parabolas is close to the value of the saddle point (12.17 kcal/mol) calculated from the grand potential. This implies that the grand potential of NO/NO^+ happens to be approximately parabolic because the dynamical change of the solute molecule is very small during the reaction. By assuming the diabatic free energy curves to be parabolic, the activation free energy shows parabolic dependence on the overpotential. The inset in Figure 2 shows the activation free energy as a function of overpotential in a wider range. It is clearly seen from the figure that the curve has approximately parabolic dependence. These results demonstrate that Marcus theory reasonably describes the present system.[43,44] However, we stress that the FTDFT/SCRF method can treat an electrochemical system in which a grand potential is far from parabolic owing to a substantial dynamical change of a solute molecule.

4.2. Exchange-Correlation Potential with Derivative Discontinuity Condition. The exchange-correlation potential was approximated by LC-BLYP in the present FTDFT approach because the conventional exchange-correlation potentials, such as B3LYP, fail to describe the derivative discontinuity with respect to the number of electrons, N.[45−47] We demonstrate in this section that the derivative discontinuity condition has a great influence on electrochemical processes in which a fractional number of electrons is allowed.

We define a reaction coordinate C approximately following the potential minimum of the NO/NO^+ 2D potential map in Figure 1. Figure 3a shows the grand potentials along the

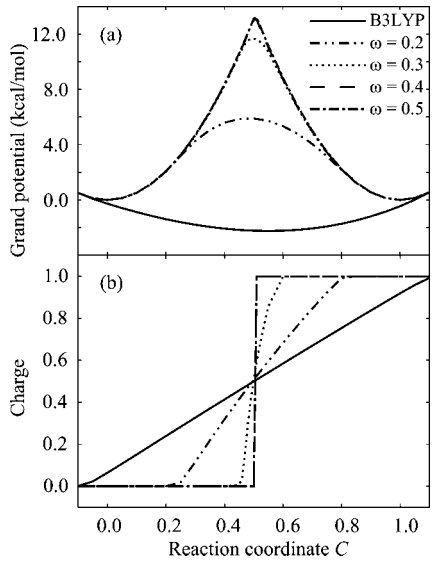

Figure 3. (a) Grand potential curves calculated with different functionals. For comparison, the grand potential curves calculated with LC-BLYP are shifted so that the grand potential at the equilibrium internuclear distance is equal to be zero. The grand potential curve calculated with B3LYP is shifted so that $E - \mu N$ is equal to be zero, where E is the total energy at the equilibrium internuclear distance obtained by the constant-N calculation. (b) Same as (a) but for the charge of the system.

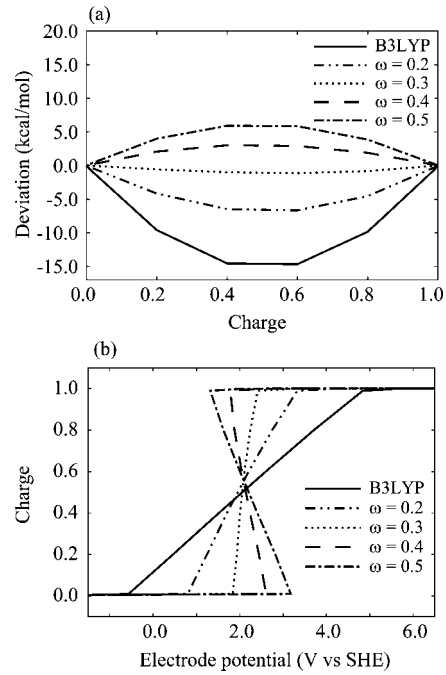

Figure 4. (a) Deviation of the energy measured from the exact one. (b) Charges as a function of the electrode potential.

coordinate C with different parameters of ω for LC-BLYP and the grand potential calculated with B3LYP. The results of LC-BLYP ($\omega = 0.2$) and B3LYP show a low or no barrier. Although the results of LC-BLYP ($\omega = 0.4$ and 0.5) show barriers, the calculations sometimes do not give the state that minimizes the grand potential at near the saddle point. Figure 3b shows the change of the charge in the NO/NO^+ electrochemical system. The charge varies strongly depending on the functional. The results of LC-BLYP ($\omega = 0.2$) and B3LYP show gradual dependence, whereas the results of LC-BLYP ($\omega = 0.4$ and 0.5) show a discontinuous change. As discussed below, the discrepancy of the grand potentials with different functionals is attributed to how each functional describes the electronic structure with the fractional number of the electrons, particularly at near the saddle point.

The functional dependence of the grand potential is strongly related to the derivative discontinuity of the energy with respect to the total number of electrons. It has been known that the exact energy should show linear dependence on N in the range of the fractional N. To demonstrate how the calculated results deviate from the exact linear dependence, we show in Figure 4a the deviation of the computed results from the energy obtained by linearly interpolating the energies of the neutral and cationic states. Then, the exact result should be zero irrespective of the charge. As expected, the dotted line of LC-BLYP ($\omega = 0.3$) depends almost linearly on N. The results of B3LYP and LC-BLYP ($\omega = 0.2$) show concave curves, whereas the results of LC-BLYP ($\omega = 0.4$ and 0.5) show convex curves. As the result, the B3LYP and LC-BLYP ($\omega = 0.2$) calculations give lower energy for the state with fractional N. This is the reason that the lower activation free energy was obtained in Figure 3a and that the number of electrons is fractional in Figure 3b. On the other hand, the LC-BLYP functionals with $\omega = 0.4$ and 0.5 give rise to another problem. Figure 4b shows the charge as a function of the electrode potential. It is clearly seen from the figure that the curves for $\omega = 0.4$ and 0.5 become triple-valued functions against the electrode potential. As mentioned in the computational details in section 3, these triple valued curves were due to a practical problem in computation. One of the three electronic states minimizes the grand potential, whereas the other two states have no physical meaning.

These behaviors are understood by considering the expressions of the exchange energy. It has been known that the Hartree−Fock approximation tends to give convex curves of the energy with respect to N, whereas the approximations used in DFT such as the local density approximation and the generalized gradient approximation tend to give concave ones. In the mixing schemes, such as B3LYP, the exchange energy is expressed as a mixture of the HF and DFT exchange energies. As shown in Figure 4a, the B3LYP calculation totally fails to reproduce the derivative discontinuity because the functional has a minor contribution from the HF exchange energy. However, if the contribution of the HF exchange energy is added more in the calculation, the obtained results will be worse in accuracy. In the LC-BLYP functional, the exchange energy in the short-range part is calculated by the BLYP functional, and the energy in the long-range part is calculated by the HF exchange potential. Since larger ω decomposes the Coulomb operator at a shorter point, the calculation with larger ω gives a convex curve, and vice versa as shown in Figure 4a. The parameter ω was finally optimized to be $\omega = 0.31$. The calculated results with $\omega = 0.31$ properly represent the derivative discontinuity and give the single-valued N as a function of the electrode potential. The value of ω optimized for the present system is close to those empirically optimized in the DFT calculations of molecules.[33−35]

5. Concluding Remarks

We have developed a computational method to calculate the electronic structures of a molecule at a constant chemical potential in the electrochemical environment. The method is based on our recently developed FTDFT approach combined with a continuum model. In the present study, the solvent effect was explicitly treated at the level of the extended SCRF model, which allows considering a nonequilibrium solvation effect.

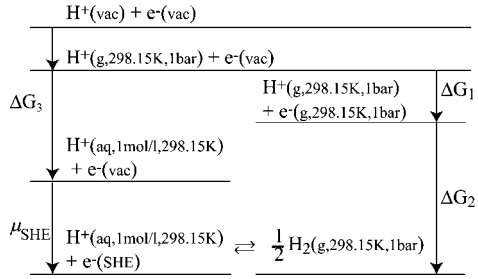

Figure 5. Born−Harber cycle to define the value of μ_{SHE}.

Furthermore, we adopted an exchange-correlation functional satisfying the derivative discontinuity condition. The FTDFT/SCRF method was applied to the electrochemical reaction of $NO^+ + e^- \rightleftarrows NO$. Owing to the improvement in the solvation effect and the exchange-correlation functional, the calculated result was in good agreement with the experimental one. The conventional exchange-correlation functional such as B3LYP does not satisfy the derivative discontinuity condition, so that the calculated result gave a completely inaccurate grand potential surface. In contrast, the functional with the long-range correction of the exchange-correlation potential has overcome the disadvantage.

Since our FTDFT method has nothing to do with theoretical levels of description of the solvent effect, the method can be straightforwardly extended to more real electrochemical systems by using sophisticated methods describing the solvent effect. In the present study, by using the extended SCRF model, we approximately described the nonequilibrium solvation effect, which was completely ignored in our previous method of FTDFT/C-PCM.

Many theoretical studies of electrochemical reactions ignore the internal degrees of freedom of a reactant. However, the geometry of the reactant, in general, strongly changes during electrochemical reaction. The present FTDFT approach allows considering the internal degrees of freedom of a reactant. Therefore, the FTDFT approach can be a suitable and promising approach to analyze the electrochemical reaction.

Acknowledgment. We are grateful to Professor R. Akiyama for helpful and fruitful discussions. This work was supported by the Grant-in-Aid (No. 18066019) and by the Next-Generation Integrated Nanoscience, "Development & Application of Advanced High-Performance Supercomputer" Project, MEXT, Japan.

Appendix A: Relationship between Chemical Potential and Electrode Potential

μ and ν are related by[48,49]

$$\nu = -\frac{\mu - \mu_{SHE}}{e} \tag{22}$$

where μ_{SHE} is the chemical potential of the electron in SHE. To compare the calculated results with experimental ones, the value of μ_{SHE} is needed. Let us consider the following equilibrium condition in SHE:

$$H^+(aq, 1\ mol/L) + e^- \rightleftarrows \frac{1}{2}H_2(gas, 1\ bar) \tag{23}$$

Then, μ_{SHE} is obtained by using the Born−Harber cycle shown in Figure 5

$$\mu_{SHE} = \Delta G_1 + \Delta G_2 - \Delta G_3 \tag{24}$$

where ΔG_1, ΔG_2, and ΔG_3 are defined in Figure 5. According to the Fermi−Dirac statistics, ΔG_1 is set to be −0.868 kcal/mol.[50] ΔG_2 is calculated to be −361.7 kcal/mol from the experimental formation energy of H^+(gas, 1 bar, 298.15 K) following the electron convention based on the Fermi−Dirac statistics.[50] The solvation energy of the hydrogen ion can be evaluated in two ways: one includes the energy to transfer the ion across the solvent surface and the other does not. In the dielectric continuum model, the solvent is treated as an infinite continuum, so that to compare the calculated results with the corresponding experiment ones the energy to penetrate the solvent surface should not be included in the solvation energy. Thus, we use the solvation energy of $\Delta G_3 = -262.1$ kcal/mol excluding the energy to penetrate the surface.[51−53] From eq 24, μ_{SHE} is finally given by

$$\mu_{SHE} = -0.868 - 361.7 + 262.1\ \text{kcal/mol} \simeq -100.47\ \text{kcal/mol} \simeq -4.36\ \text{eV} \tag{25}$$

This value is similar to those obtained by other authors, −4.31 eV,[48] −4.34 eV,[49] and −4.36 eV.[52] From eq 22, the electrode potential is given by

$$\nu = -\frac{\mu}{e} - 4.36\ \text{V vs SHE} \tag{26}$$

Appendix B: Derivation of ΔE in Equation 14

The energy difference ΔE is calculated by $\Delta E = V_{int} + W_{pol}$, where V_{int} is the electrostatic interaction energy between the molecule and the dielectric and W_{pol} is the work required to polarize the dielectric. In the SCRF model, V_{int} up to the dipole term can be expressed as[23]

$$V_{int} = q\phi(0) + \mathbf{m} \cdot \nabla\phi(0) \tag{27}$$

where $\phi(0)$ is the electrostatic potential at the center of the cavity. Let us first consider an equilibrium solvation model. On the assumption that the system is in a spherical dielectric cavity, the electrostatic field and its derivative are expressed as

$$\phi(0) = -f_q^{\,0} q \tag{28}$$

$$\nabla\phi(0) = -f_m^{\,0}\mathbf{m} \tag{29}$$

where $f_q^{\,0}$ and $f_m^{\,0}$ are the reaction field factors for the charge and the dipole moment. The reaction field factors are explicitly given by

$$f_q^{\,0} = \left(1 - \frac{1}{\varepsilon_0}\right)\frac{1}{a_0} \tag{30}$$

$$f_m^{\,0} = \frac{2(\varepsilon_0 - 1)}{2\varepsilon_0 + 1}\frac{1}{a_0^3} \tag{31}$$

where a_0 is the radius of the cavity and ε_0 is the dielectric constant. By substituting eqs 28 and 29 into eq 27, the electrostatic interaction energy is rewritten in the form of

$$V_{int} = -f_q^{\,0} q^2 - f_m^{\,0}\mathbf{m} \cdot \mathbf{m} \tag{32}$$

By using the reaction field factors, W_{pol} and ΔE are expressed as[23]

$$W_{pol} = \frac{1}{2}f_q^{\,0} q^2 + \frac{1}{2}f_m^{\,0}\mathbf{m} \cdot \mathbf{m} \tag{33}$$

$$\Delta E = -\frac{1}{2}f_q^{\,0} q^2 - \frac{1}{2}f_m^{\,0}\mathbf{m} \cdot \mathbf{m} \tag{34}$$

Equations 32 and 33 satisfy the condition, $\Delta E = V_{int} + W_{pol}$.

Let us next consider a nonequilibrium solvation model.[23,24] With the help of the relationship between the dielectric constant

ε and the refractive index n, $\varepsilon = n^2$, for optical processes, we introduce the quantities of

$$f_q^{\infty} = \left(1 - \frac{1}{n^2}\right)\frac{1}{a_0} \tag{35}$$

$$f_m^{\infty} = \frac{2(n^2-1)}{2n^2+1}\frac{1}{{a_0}^3} \tag{36}$$

where f_q^{∞} and f_m^{∞} are the reaction field factors of the short-lived components for the charge and the dipole moment, respectively. The reaction fields $\phi_s(0)$ and $\nabla\phi_s(0)$ produced by the short-lived component of the polarization are given by

$$\phi_s(0) = -f_q^{\infty} q \tag{37}$$

$$\nabla\phi_s(0) = -f_m^{\infty}\mathbf{m} \tag{38}$$

When deriving these equations, we suppose that the short-lived component of the polarization is induced by a charge q and a dipole moment $\mathbf{m}$. On the other hand, the long-lived component is assumed to be induced by a charge q^0 and a dipole moment $\mathbf{m}^0$. Then, the reaction fields $\phi_l(0)$ and $\nabla\phi_l(0)$ produced by the long-lived component of the polarization are obtained by subtracting the short-lived component as follows:

$$\phi_l(0) = -(f_q^{\,0} - f_q^{\infty})q^0 \tag{39}$$

$$\nabla\phi_l(0) = -(f_m^{\,0} - f_m^{\infty})\mathbf{m}^0 \tag{40}$$

By combining the reaction fields produced by the short-lived and the long-lived components, the total reaction fields $\phi(0)$ and $\nabla\phi(0)$ are obtained by

$$\phi(0) = -(f_q^{\,0} - f_q^{\infty})q^0 - f_q^{\infty} q \tag{41}$$

$$\nabla\phi(0) = -(f_m^{\,0} - f_m^{\infty})\mathbf{m}^0 - f_m^{\infty}\mathbf{m} \tag{42}$$

The potential energy V_{int} is given by substituting eqs 41 and 42 into eq 27,

$$V_{\mathrm{int}} = -q[(f_q^{\,0} - f_q^{\infty})q^0 + f_q^{\infty} q] - \mathbf{m}\cdot[(f_m^{\,0} - f_m^{\infty})\mathbf{m}^0 + f_m^{\infty}\mathbf{m}] \tag{43}$$

In a manner analogous to eq 33, the work $W_{\mathrm{pol}}{}^{\mathrm{s}}$ required to polarize the short-lived component, which is induced by q and $\mathbf{m}$, is given by

$$W_{\mathrm{pol}}{}^{\mathrm{s}} = \frac{1}{2}[f_q^{\infty} q^2 + f_m^{\infty}\mathbf{m}\cdot\mathbf{m}] \tag{44}$$

The work $W_{\mathrm{pol}}{}^{\mathrm{l}}$ required to polarize the long-lived component, which is induced by q^0 and $\mathbf{m}^0$, is obtained by

$$W_{\mathrm{pol}}{}^{\mathrm{l}} = \frac{1}{2}[f_q^{\,0}(q^0)^2 + f_m^{\,0}\mathbf{m}^0\cdot\mathbf{m}^0] - \frac{1}{2}[f_q^{\infty}(q^0)^2 + f_m^{\infty}\mathbf{m}^0\cdot\mathbf{m}^0] \tag{45}$$

where the first term is the work required to polarize both the long-lived and the short-lived components induced by q^0 and $\mathbf{m}^0$ and the second term is the work required to polarize the short-lived component induced by q^0 and $\mathbf{m}^0$. The work $W_{\mathrm{pol}} = W_{\mathrm{pol}}{}^{\mathrm{s}} + W_{\mathrm{pol}}{}^{\mathrm{l}}$ required to polarize the dielectric is given by

$$W_{\mathrm{pol}} = \frac{1}{2}[(f_q^{\,0} - f_q^{\infty})(q^0)^2 + f_q^{\infty} q^2 + (f_m^{\,0} - f_m^{\infty})\mathbf{m}^0\cdot\mathbf{m}^0 + f_m^{\infty}\mathbf{m}\cdot\mathbf{m}] \tag{46}$$

Finally, ΔE is obtained by

$$\Delta E = V_{\mathrm{int}} + W_{\mathrm{pol}} = \frac{1}{2}(f_q^{\,0} - f_q^{\infty})(q^0)^2 - \frac{1}{2}f_q^{\infty} q^2 - (f_q^{\,0} - f_q^{\infty})q(q^0) + \frac{1}{2}(f_m^{\,0} - f_m^{\infty})\mathbf{m}^0\cdot\mathbf{m}^0 - \frac{1}{2}f_m^{\infty}\mathbf{m}\cdot\mathbf{m} - (f_m^{\,0} - f_m^{\infty})\mathbf{m}\cdot\mathbf{m}^0 \tag{47}$$

This equation is equivalent to eq 14.

Appendix C: Finite-Temperature KS Equation with the SCRF Model

The charge and the dipole moment can be divided into the components associated with electrons (e) and nuclei (n):

$$q = q_{\mathrm{e}} + q_{\mathrm{n}} \tag{48}$$

$$\mathbf{m} = \mathbf{m}_{\mathrm{e}}\frac{q_{\mathrm{e}} - q}{q_{\mathrm{e}}} + \mathbf{m}_{\mathrm{n}} \tag{49}$$

In the present FTDFT calculation, q_{e}, q_{n}, $\mathbf{m}_{\mathrm{e}}$, and $\mathbf{m}_{\mathrm{n}}$ are defined by

$$q_{\mathrm{e}} = \sum_i f_i \int \psi_i^*(\mathbf{x})\hat{q}\psi_i(\mathbf{x})\,\mathrm{d}\mathbf{x} \tag{50}$$

$$\mathbf{m}_e = \sum_i f_i \int \psi_i^*(\mathbf{x})\hat{\mathbf{m}}\psi_i(\mathbf{x})\,\mathrm{d}\mathbf{x} \tag{51}$$

$$q_{\mathrm{n}} = \sum_j Q_j \tag{52}$$

$$\mathbf{m}_{\mathrm{n}} = \sum_j \mathbf{R}_j Q_j \tag{53}$$

where Q_j and $\mathbf{R}_j$ are the charge and the position of the jth nucleus, respectively. The dipole moment (eq 49) is evaluated at the center of the electric charge because the dipole moment depends on the origin of the coordinate.[54] Substituting eqs 50−53 into eq 14 and then performing the functional derivative of ΔE with respect to $\psi_i^*(\mathbf{x})$, we obtain eq 18

$$v_{\mathrm{scrf}} = -[f_q^{\infty} q\hat{q} + (f_q^{\,0} - f_q^{\infty})q^0\hat{q} + f_m^{\infty}\mathbf{m}\cdot\hat{\mathbf{m}} + (f_m^{\,0} - f_m^{\infty})\mathbf{m}^0\cdot\hat{\mathbf{m}}] \tag{54}$$

References and Notes

(1) Bard, A. J.; Faulkner, L. R. *Electrochemical Methods: Fundamentals and Applications*; John Wiley & Sons: New York, 1980.
(2) Bockris, J. O'M.; Khan, S. U. M. *Surface electrochemistry*; Plenum: New York, 1993.
(3) Tavernelli, I.; Vuilleumier, R.; Sprik, M. *Phys. Rev. Lett.* **2002**, *88*, 213002.
(4) Blumberger, J.; Bernasconi, L.; Tavernelli, I.; Vuilleumier, R.; Sprik, M. *J. Am. Chem. Soc.* **2004**, *126*, 3928.
(5) Tateyama, Y.; Blumberger, J.; Sprik, M.; Tavernelli, I. *J. Chem. Phys.* **2005**, *122*, 234505.
(6) Blumberger, J.; Tavernelli, I.; Klein, M. L.; Sprik, M. *J. Chem. Phys.* **2006**, *124*, 064507.
(7) Anderson, A. B.; Kang, D. B. *J. Phys. Chem. A* **1998**, *102*, 5993.
(8) Anderson, A. B.; Albu, T. V. *J. Am. Chem. Soc.* **1999**, *121*, 11855.
(9) Cai, Y.; Anderson, A. B. *J. Phys. Chem. B* **2004**, *108*, 9829.
(10) Anderson, A. B.; Cai, Y.; Sidik, R. A.; Kang, D. B. *J. Electroanal. Chem.* **2005**, *580*, 17.
(11) Nakatsuji, H. *J. Chem. Phys.* **1987**, *87*, 4995.
(12) Fukunishi, Y.; Nakatsuji, H. *J. Chem. Phys.* **1992**, *97*, 6535.
(13) Nakatsuji, H.; Nakai, H. *Can. J. Chem.* **1992**, *70*, 404.
(14) Taylor, C. D.; Wasileski, S. A.; Filhol, J.-S.; Neurock, M. *Phys. Rev. B* **2006**, *73*, 165402.
(15) Lozovoi, A. Y.; Alavi, A.; Kohanoff, J.; Lynden-Bell, R. M. *J. Chem. Phys.* **2001**, *115*, 1661.
(16) Lozovoi, A. Y.; Alavi, A. *Phys. Rev. B* **2003**, *68*, 245416.
(17) Jacobi, S.; Baer, R. *J. Chem. Phys.* **2005**, *123*, 044112.
(18) Otani, M.; Sugino, O. *Phys. Rev. B* **2006**, *73*, 115407.
(19) Shiratori, K.; Nobusada, K. *Chem. Phys. Lett.* **2008**, *451*, 158.

(20) Mermin, N. D. *Phys. Rev.* **1965**, *137*, A1441.
(21) Cossi, M.; Rega, N.; Scalmani, G.; Barone, V. *J. Comput. Chem.* **2003**, *24*, 669.
(22) Perdew, J. P.; Parr, R. G.; Levy, M.; Balduz, J. L., Jr. *Phys. Rev. Lett.* **1982**, *49*, 1691.
(23) Böttcher, C. J. F *Theory of electric polarization Volume I*; Elsevier: Amsterdam, 1973.
(24) Ruiz-López, M. F.; Rinaldi, D.; Bertrán, J. *J. Chem. Phys.* **1995**, *103*, 9249.
(25) Lee, K. Y.; Kuchynka, D. J.; Kochi, J. K. *Inorg. Chem.* **1990**, *29*, 4196.
(26) Parr, R. G.; Yang, W. *Density-Functional Theory of Atoms and Molecules*; Oxford University Press: New York, 1989.
(27) Hohenberg, P.; Kohn, W. *Phys. Rev.* **1964**, *136*, B864.
(28) Kohn, W.; Sham, L. J. *Phys. Rev.* **1965**, *140*, A1133.
(29) Basilevsky, M. V.; Rostov, I. V.; Newton, M. D. *Chem. Phys.* **1998**, *232*, 189.
(30) Newton, M. D.; Basilevsky, M. V.; Rostov, I. V. *Chem. Phys.* **1998**, *232*, 201.
(31) Becke, A. D. *Phys. Rev. A* **1988**, *38*, 3098.
(32) Lee, C.; Yang, W.; Parr, R. G. *Phys. Rev. B* **1988**, *37*, 785.
(33) Iikura, H.; Tsuneda, T.; Yanai, T.; Hirao, K. *J. Chem. Phys.* **2001**, *115*, 3540.
(34) Tawada, Y.; Tsuneda, T.; Yanagisawa, S.; Yanai, T.; Hirao, K. *J. Chem. Phys.* **2004**, *120*, 8425.
(35) Song, J.-W.; Hirosawa, T.; Tsuneda, T.; Hirao, K. *J. Chem. Phys.* **2007**, *126*, 154105.
(36) Chai, J.-D.; Head-Gordon, M. *J. Chem. Phys.* **2008**, *128*, 084106.
(37) Henderson, T. M.; Janesko, B. G.; Scuseria, G. E. *J. Chem. Phys.* **2008**, *128*, 194105.
(38) Dunning, T. H., Jr. *J. Chem. Phys.* **1989**, *90*, 1007.
(39) Kendall, R. A.; Dunning, T. H., Jr.; Harrison, R. J. *J. Chem. Phys.* **1992**, *96*, 6796.
(40) *Lange's Handbook of chemistry*, 12th ed.; Dean, J. A., Ed.; McGraw-Hill: New York, 1979.
(41) Schmidt, M. W.; Baldridge, K. K.; Boatz, J. A.; Elbert, S. T.; Gordon, M. S.; Jensen, J. H.; Koseki, S.; Matsunaga, N.; Nguyen, K. A.; Su, S. J.; Windus, T. L.; Dupuis, M.; Montgomery, J. A. *J. Comput. Chem.* **1993**, *14*, 1347.
(42) Bondi, A. *J. Phys. Chem.* **1964**, *68*, 441.
(43) Kim, H. J.; Hynes, J. T. *J. Chem. Phys.* **1990**, *93*, 5194.
(44) Kim, H. J.; Hynes, J. T. *J. Chem. Phys.* **1990**, *93*, 5211.
(45) Vydrov, O. A.; Scuseria, G. E.; Perdew, J. P. *J. Chem. Phys.* **2007**, *126*, 154109.
(46) Cohen, A. J.; Mori-Sánchez, P.; Yang, W. *J. Chem. Phys.* **2007**, *126*, 191109.
(47) Cohen, A. J.; Mori-Sánchez, P.; Yang, W. *Phys. Rev. B* **2008**, *77*, 115123.
(48) Trasatti, S. *J. Chem. Soc., Faraday Trans. 1* **1974**, *70*, 1752.
(49) Llano, J.; Eriksson, L. A. *J. Chem. Phys.* **2002**, *117*, 10193.
(50) Bartmess, J. E. *J. Phys. Chem.* **1994**, *98*, 6420.
(51) Tissandier, M. D.; Cowen, K. A.; Feng, W. Y.; Gundlach, E.; Cohen, M. H.; Earhart, A. D.; Coe, J. V.; Tuttle, T. R., Jr. *J. Phys. Chem. A* **1998**, *102*, 7787.
(52) Lewis, A.; Bumpus, J. A.; Truhlar, D. G.; Cramer, C. J. *J. Chem. Educ.* **2004**, *81*, 596.
(53) This value,−262.1 kcal/mol, is the sum of the solvation energy without changing the concentration (−264.0 kcal/mol)[51] and the work to change the state of the ideal gas from 1 bar to 1 mol/L (1.90 kcal/mol).[52]
(54) Wong, M. W.; Frisch, M. J.; Wiberg, K. B. *J. Am. Chem. Soc.* **1991**, *113*, 4776.

JP803923F